THE JOURNAL OF PHYSICAL CHEMISTRY B

Article

pubs.acs.org/JPCB

RNA Polymerase II Subunits Exhibit a Broad Distribution of Macromolecular Assembly States in the Interchromatin Space of Cell Nuclei

Michael A. Tycon, Matthew K. Daddysman, and Christopher J. Fecko*

Department of Chemistry, University of North Carolina at Chapel Hill, Chapel Hill, North Carolina 27599-3290, United States

Supporting Information

ABSTRACT: Nearly all cellular processes are enacted by multi-subunit protein complexes, yet the assembly mechanism of most complexes is not well understood. The anthropomorphism "protein recruitment" that is used to describe the concerted binding of proteins to accomplish a specific function conceals significant uncertainty about the underlying physical phenomena and chemical interactions governing the formation of macromolecular complexes. We address this deficiency by investigating the diffusion dynamics of two RNA polymerase II subunits, Rpb3 and Rpb9, in regions of live *Drosophila* cell nuclei that are devoid of chromatin binding sites. Using FRAP microscopy, we demonstrate that both unengaged subunits are incorporated into a broad distribution of complexes, with sizes ranging from free (unincorporated) proteins to those that have been predicted for fully assembled gene transcription units. In live cells, Rpb3 exhibits regions of stability at both size extremes connected by a continuous distribution of complexes. Corresponding measurements on cellular extracts reveal a distribution that retains peaks at the extremes but not in between, suggesting that partially assembled complexes are less stable. We propose that the broad distribution of macromolecular species allows for mechanistic flexibility in the assembly of transcription complexes.

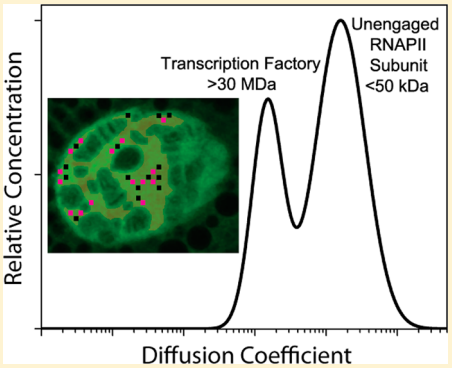

INTRODUCTION

A central question in modern molecular biology is the mechanism by which large, multi-subunit protein complexes assemble inside a cell. Essential cellular processes such as transcription,[1] splicing,[1,2] and genome repair[3] are undertaken by massive assemblies involving many distinct molecular modules that efficiently carry out specific tasks. Protein recruitment, the initial step in assembly, is often viewed as a "black box", as molecular-level details about transport phenomena and macromolecular associations involved in this process remain ambiguous.[4] Two primary models have emerged to explain how cellular machinery assembles to handle the dynamic demands they must meet.[5] One proposal is a top-down approach, in which the components of a macromolecular assembly bind one another prior to receiving an activation signal, forming a stable supra-assembly that is often called a molecular factory. Such a factory would be poised for efficient handling of cellular tasks but would be slow to traverse the cellular interior and poorly suited to respond to changing external stimuli. On the other extreme is a bottom-up approach, in which each component of the final molecular assembly diffuses through the cellular interior individually and stochastically encounters binding partners at the active site until the entire complex is amassed. This stochastic model would enable rapid movement of the smaller molecular modules within the cell, but the binding steps to form a full complex from individual components may limit the overall activation rate. Interestingly, proponents of both models invoke the crowded nuclear milieu as corroborating evidence, either in support of factory domains or restrictive nuclear architecture.[6,7] In an effort to distinguish between these paradigms, we decided to investigate the incorporation of individual components of the RNA polymerase II (RNAPII) transcription complex in regions of live cell nuclei devoid of chromatin binding sites.

The present study specifically investigates RNAPII, since it is responsible for mRNA production and occupies a critical position in the central dogma.[8−11] While extensive *in vitro* molecular biology research has elucidated the mechanical intricacies of how the RNAPII complex transcribes template DNA, the advent of *in vivo* fluorescent labeling and the widespread use of fluorescent microscopy have enabled detailed observations of RNAPII complex interactions with chromatin in the native cellular environment.[12−15] Much work has been conducted to characterize RNAPII behavior in bacterial, insect, and mammalian systems; however, the majority focuses specifically on subunit assembly and interactions on chromatin, typically in the vicinity of DNA binding sequences. In studies using both RNAPI and RNAPII, polymerase subunits and transcription factors have been found to have distinct dynamics, arguing against preassembled complexes,[12,13,16] though these

Received: August 19, 2013
Revised: December 16, 2013
Published: December 19, 2013

results contradict some earlier work.[17−19] Further, it remains unresolved whether the assembly is stochastic[13] or stepwise,[12,20] with implications for a generalized framework of multicomponent protein assemblies.[21]

No previous investigations have characterized RNAPII component diffusion dynamics preceding chromatin interactions in cells, and most studies have completely neglected the importance of diffusion. We postulated that measuring the diffusion dynamics of RNAPII components prior to chromatin binding could yield insights into the mode of assembly. We sought to better understand the process of RNAPII complex assembly and nuclear mobility by investigating the dynamics of the third and ninth subunits of RNAPII (Rpb3 and Rpb9) in the interchromatin space (nucleoplasm devoid of chromatin) of cell nuclei using fluorescence recovery after photobleaching (FRAP).[22]

We express fusions of Rpb3 and Rpb9, two subunits exclusive to RNAPII, with enhanced green fluorescent protein (GFP) in the polytene cells of *Drosophila melanogaster* larvae.[23] These polytene cells contain many copies of the genomic DNA that form large chromosomal bundles during interphase (Figure 1a,b).[24] By expressing RNAPII subunit-GFP fusions and H2B-mRFP tagged histones in polytene cells, we are able to optically resolve nuclear regions containing chromatin and restrict our analysis exclusively to the interchromatin space (Figure 1). This region is devoid of chromatin and therefore lacks DNA binding sites. We find the diffusion of both RNAPII subunits was non-Brownian and the recovery dynamics of the two subunits are different.

While non-Brownian diffusive behavior is often termed anomalous and attributed to molecular crowding,[25] we propose a fundamentally different interpretation. Through a comparison to the mobility of unconjugated GFP (lacking a localization sequence),[26] which does exhibit Brownian diffusion, we determine that molecular crowding is not responsible for the observed diffusive behavior. Rather, both RNAPII subunits must participate in heterogeneous distributions of complexes with a broad range of sizes, from isolated subunits to fully assembled transcription complexes. We term this type of diffusive behavior *apparent anomalous diffusion,* in which non-Brownian behavior is observed by simultaneously probing many states of preformed complexes with different diffusion coefficients.

RESULTS

1. Automated "Shotgun ptFRAP" Data Collection. We chose to study the transport properties of the RNAPII subunits Rpb3 and Rpb9 in the absence of chromatin binding sites or membrane perturbations by restricting the region of FRAP investigation to the interchromatin space of cell nuclei. We used a point-FRAP (ptFRAP) method to probe diffusion, which is an implementation where optical diffraction-limited spots are photobleached and the fluorescent recovery tracked in time with sub-millisecond resolution.[26] In contrast to the more common area-FRAP in which micrometer-sized features are photobleached,[27] ptFRAP probes smaller sample regions and enables several orders of magnitude higher time resolution. To restrict the analysis of photobleaching recovery to the interchromatin space of polytene nuclei (avoiding both cellular membranes and chromatin regions) and prevent data points from overlapping in space during collection, we implemented an automated data point collection method termed "shotgun ptFRAP" (Figure 1). As the primary limitation of the ptFRAP

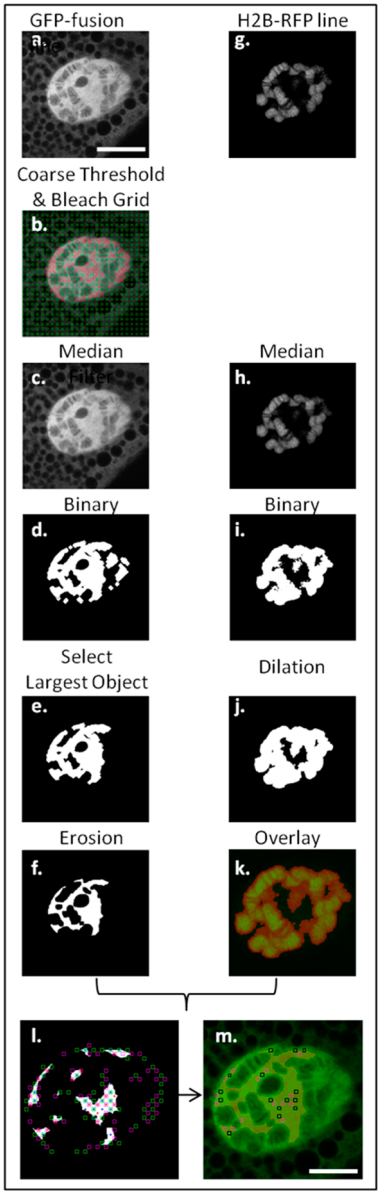

Figure 1. Image collection and automated processing methodology "shotgun ptFRAP": (a, g) An initial image of both color channels is captured and used in subsequent thresholding operations. The GFP channel corresponds to the protein of interest and the RFP channel to the labeled polytene chromosomes. (b) A grid with 2 μm spacing is applied to the entire field of view. These grid points define the positions where FRAP data is collected. A coarse threshold is applied to the GFP channel; only grid points contained within the thresholded region are collected (magenta boxes). Alternating points of the grid correspond to bleach and control data points. Postprocessing steps are performed using MATLAB scripts developed in-house. (c, h) After data collection, a median filter is applied to both images to remove noise. (d, i) Threshold values are carefully selected for each image to capture the contours of the nuclear features. (e, f) In the GFP channel, the largest object in the field of view, corresponding to the nucleus, is retained. This eliminates any contributions from cytoplasmic signal. The binary mask is processed to remove sharp edge features and then eroded 500 nm from every periphery to eliminate grid points in the vicinity of cellular membranes. (j) The polytene binary mask is dilated 300 nm to remove any grid points near the chromatin. (k) The mask (red can be seen overlaid with the image) confirms the entire region containing the polytenes will be excluded from analysis. (l, m) The RFP channel mask is subtracted from the GFP channel mask; the resulting region corresponds to the interchromatin space. The open

dx.doi.org/10.1021/jp4082933 | J. Phys. Chem. B 2014, 118, 423−433

Figure 1. continued

squares (green = control power, magenta = bleach power) indicate all grid points at which FRAP data is collected during the experiment, while squares enclosing dots indicate the grid points retained for analysis. The distributions of the retained grid points are inspected visually to verify the selection criteria have been met. Scale bar, 10 μm.

method is the low SNR resulting from photon collection from a minuscule volume, signal averaging over hundreds of individual bleach and control points is required. Collecting sufficient data within the lifetime of the dissected samples (~1 h) and in a manner to avoid user-selection bias necessitated an automated collection method. In our implementation, an image of the sample is collected followed by the collection of ptFRAP curves at evenly spaced grid points across the entire sample. The method consists of a data collection program in which evenly spaced data points are collected across the entire cell nuclei (i.e., the entire cell is "hit", Figure 1b), followed by a postexperiment screening step that retains only data points in regions of interest that match our selection criteria (Figure 1l,m). The grid points are spaced by 2 μm, sufficiently far apart to avoid any overlapping bleach volumes, as the axial extent of the PSF is only 300 nm. Thus, all regions of the nuclei are probed over the course of the experiment and individual regions can be analyzed afterward. This procedure enables over a thousand data points to be collected in under an hour, without user bias, and they are averaged into a single FRAP data set.

2. RNAPII Subunits Exhibit Apparent Anomalous Diffusion in Cells. Rpb3 is the third largest RNAPII subunit, having a native mass of 35 kDa; the GFP-fusion construct has a mass of 62 kDa. Native Rpb9 is less massive at 14 kDa; the fusion construct has a mass of 41 kDa. Both tagged subunits are incorporated into active transcription complexes,[28] and the subunits have high binding affinities for most of the 10 remaining RNAPII subunits.[29] Additionally, RNAPII has strong affinities for transcription factors and promoter proteins, giving rise to a large distribution of complexes in which Rpb3 and Rpb9 may participate. Using the ptFRAP method, we compared the recovery dynamics of both subunits in the interchromatin space of polytene nuclei, which were then compared to the recovery of unconjugated GFP under the same conditions. The GFP acts as an inert protein with no binding partners in the nucleus and is only subject to molecular crowding (Figure 2).

We have previously shown that unconjugated GFP obeys Brownian diffusion in the interchromatin space,[26] exhibiting a reduced diffusion coefficient due to nuclear viscosity. For this study, GFP serves as an approximate molecular mass standard to account for the effects of nuclear crowding as a reduction in the translational diffusion coefficient.[30] However, it is apparent that differences in the FRAP curves between the RNAPII subunits and GFP (Figure 2c) indicate that the transport of these former species is not well described by Brownian diffusion. This result is striking given the similar masses of the three proteins and the weak dependence of diffusional mobility with molecular mass predicted by the Stokes–Einstein equation.

Given the large differences between the recovery of GFP and the RNAPII subunits, we chose to initially fit the Rpb3 and Rpb9 FRAP curves with a model that allows for anomalous subdiffusion. Anomalous subdiffusion equations are often

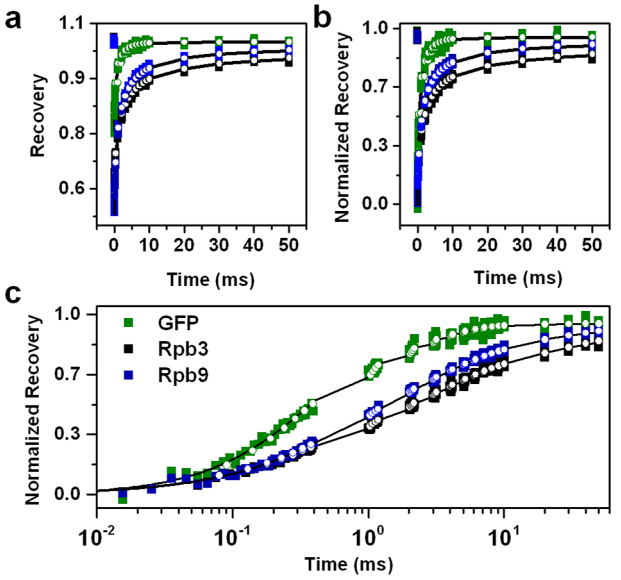

Figure 2. Comparison of *in vivo* subunit recovery dynamics: (a) The FRAP curves for the unconjugated GFP (green), the Rpb3-GFP (black), and Rpb9-GFP (blue) are shown. Data are plotted as closed squares, the best fits to an anomalous diffusion model are shown as black lines, and the best fits to the distribution model are shown as white circles. The data was collected with an intermittent collection technique that minimizes photobleaching while enabling long-duration interrogation. Numerous FRAP curves were averaged for each sample (GFP-1505 pts, Rpb3-1694 pts, Rpb9-833 pts) to achieve a high SNR. All displayed data has been treated to a 10-point rolling average smooth to aid clarity, but all fitting was performed on the untreated data sets starting at the 80 μs time point. (b) Evident from the immediate postbleach data point, each protein exhibits a different bleach depth. This reflects a sample-specific protein expression level effect that significantly influences the bleach depth. To enable a qualitative comparison of the FRAP recovery curves, we normalized the FRAP bleach depth for each sample to zero. The rescaled FRAP curves clearly indicate differences between the recovery profiles of GFP, Rpb3, and Rpb9. The recovery differences are striking given the similar molecular masses and identical nuclear environment. (c) For better comparison of short-time data, the rescaled recovery curves are displayed on a logarithmic time axis. Here, the differences in the slopes of recovery curves can be visualized: the flatter the slope, the greater the apparent anomaly factor.

invoked to describe mass transport in which the mean squared displacement of each particle is sublinear with time, which can result from heterogeneity in the molecular environment:

$$\langle \Delta r^2 \rangle = 6\frac{\Gamma}{\alpha}t^{\alpha} \quad (1)$$

The particle displacement is Δr, Γ is the transport coefficient, t is the time interval, and α is the anomaly value. The principle parameter describing anomalous diffusion is the anomaly value, bound between zero and unity, which indicates the magnitude of the deviation from Brownian behavior. An anomaly factor of unity corresponds to Brownian behavior (for which the transport coefficient is the diffusion coefficient); smaller values indicate progressively larger deviations. Such hindered molecular motion is often attributed to intracellular factors that retard the motion of a particle, such as binding to immobile traps, participation in viscoelastic complexes, and physical obstruction through labyrinthine corralling.[31]

The ptFRAP model previously developed by our group[26] accounts for both anomalous diffusion[32] and a reversible

dx.doi.org/10.1021/jp4082933 | J. Phys. Chem. B 2014, 118, 423–433

photobleaching correction due to dark-state transitions of GFP during data collection. The FRAP signal is

$$F(t) = F_0\left[1 + \delta \exp\left(\frac{-t_{laser}}{\tau_{pp}}\right)\right] \times \sum_{n=0}^{\infty} \frac{(-\beta)^n}{n!}\left[1 + n\left(1 + \frac{16\Gamma t^{\alpha}}{\alpha\omega_r^{\,2}}\right)\right]^{-1} \times \left[1 + n\left(1 + \frac{16\Gamma t^{\alpha}}{\alpha\omega_z^{\,2}}\right)\right]^{-1/2} \quad (2)$$

Here, F_0 is the prebleach fluorescence intensity, β is a factor related to the bleach depth, δ and t_{laser} are the reversible bleaching magnitude and time scale, and ω_r and ω_z are the size of the focused Gaussian beam in the radial and axial dimensions, respectively. All of our data exhibited a near complete recovery on the 50 ms time scale, indicating no immobile fractions. We fit the averaged FRAP curves according to eq 2 (Figure 2, black lines, see Supplementary Table 1 (Supporting Information) for fit parameters from individual data sets); the best fit parameters are compared (Figure 3).

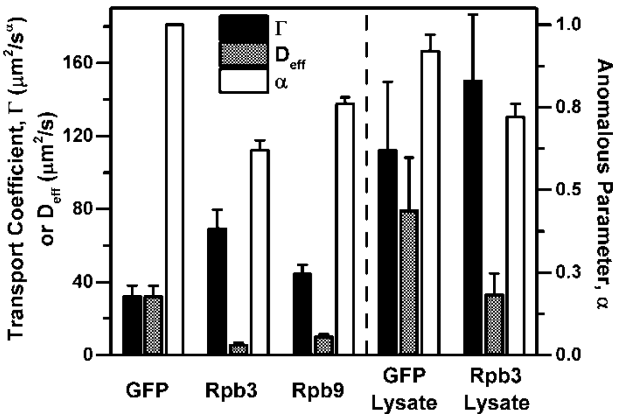

Figure 3. Summary of the best-fit apparent anomalous modeling parameters: The alpha value varies between zero and unity and is a measure of deviation from Brownian diffusion. The transport coefficient is a measure of translational diffusion speed, and the effective diffusion coefficient (D_{eff}) represents the normal diffusion coefficient corresponding to the $^1/_2$ FRAP recovery time of the anomalous particle if it had diffused normally. Error bars are shown at the 95% confidence interval. The GFP expressing line was found to diffuse normally with a diffusion coefficient of 32 ± 6 $\mu m^2/s$. The RNAPII subunits showed apparent anomalous diffusion, with each exhibiting different diffusive kinetics. Rpb3 exhibited an apparent anomaly value of 0.62 ± 0.03, while Rpb9 exhibited an anomaly value of 0.76 ± 0.02. This reveals that the subunits are not bound in identical complexes. To the right of the dotted line are the parameters for the *in vitro* lysate experiments. Within experimental error, the diffusion of GFP is found to be Brownian and of the same magnitude as GFP in dilute buffer. The Rpb3 lysate continues to indicate apparent anomalous diffusion.

We found that both RNAPII subunit recoveries were well fit by the anomalous subdiffusion model. This is in contrast to the GFP recovery dynamics which were well fit by Brownian diffusion.[26] Since our GFP experiments have revealed that molecular crowding is not a source of anomalous diffusion and these experiments restricted the analysis to an identical nuclear environment devoid of RNAPII binding sites or membrane induced labyrinthine regions, we can infer that the observed subunit recovery is not true anomalous diffusion.

As another possible source of observed anomalous behavior, we considered that the simultaneous measurement of multiple diffusing species (a distribution) undergoing Brownian motion can produce an identical FRAP recovery profile to a single species undergoing anomalous diffusion.[33] We term this phenomenon *apartment anomalous diffusion*. Thus, we strongly believe that the subunits must be in a heterogeneous distribution of complexes resulting in the observation of apparent anomalous diffusion, as described in section 4.

3. Rpb3 Exhibits Apparent Anomalous Diffusion in Cell Lysate. We reasoned if the apparent non-Brownian transport persisted in dilute solution then the deviations from Brownian diffusion must be attributed to a distribution of complexes. To completely eliminate macromolecular crowding as a possible source of anomalous diffusion, we performed FRAP experiments on cellular lysates of the salivary gland polytene cells expressing either GFP or Rpb3 (Figure 4).

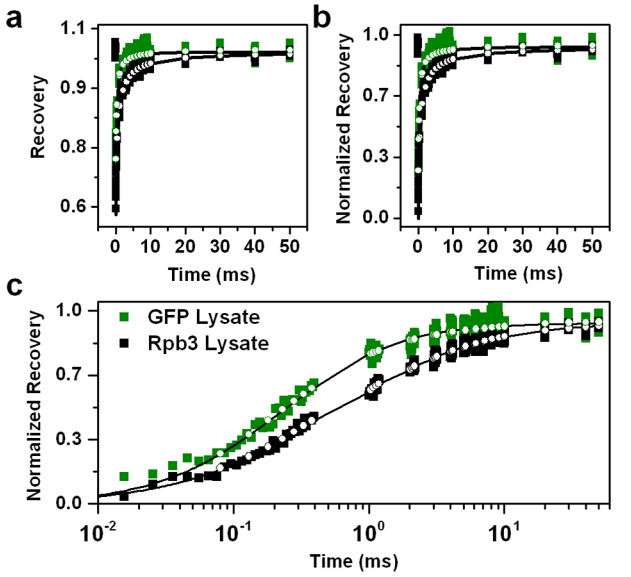

Figure 4. Comparison of *in vitro* subunit recovery dynamics: The FRAP curves for the GFP expressing control line and the Rpb3 subunit lysate experiments are shown. Numerous FRAP curves were averaged for each sample due to the low signal intensity of the lysates (GFP - 6090 pts, Rpb3 - 17420 pts). (a–c) Data are plotted as closed squares, the best fits to an anomalous diffusion model are shown as black lines, and the best fits to the distribution model are shown as white circles. (c) The flattened slope and slower recovery of the Rpb3 lysate is a clear indication that the sample is not undergoing Brownian diffusion.

The cell lysates are whole cell preparations made by sonicating the salivary glands in a lysis buffer and extracting the soluble proteins. The cell contents were centrifuged and the supernatant used for FRAP experiments. A comparison of the fluorescent intensity between the lysates and the intact polytene cells revealed up to a 30-fold decrease in signal. We were unable to collect data on lysates made from Rpb9 due to extremely low sample signal.

The GFP lysate FRAP recovery indicated a normally diffusing species (Figure 4). Further, the diffusion coefficient determined by the FRAP model described in eq 2 of 79.1 ± 30.0 $\mu m^2/s$ is in excellent agreement with the diffusion of free

dx.doi.org/10.1021/jp4082933 | J. Phys. Chem. B 2014, 118, 423–433

GFP (purified from bacteria) in solution, measured on our setup as 84 ± 6 $\mu m^2/s$.[20] Thus, our lysate preparation recapitulated a dilute solute environment by eliminating macromolecular crowding. We note that the GFP lysate yielded a slightly non-Brownian anomaly parameter (Figure 3), which is the result of the very rapid recovery of the species coupled with low signal strength. Both of these factors reduce the accuracy and precision of the fitting algorithm.

Despite the highly dilute solvent environment, the Rpb3 lysate FRAP recovery reveals very different behavior (Figure 4), displaying apparent anomalous diffusion (Figure 3). Due to the lower viscosity of the lysate solvent, both the transport and effective diffusion coefficients, determined by eq 1, are increased compared to Rpb3 diffusion *in vivo*. Further, the lysate recovery is slightly less anomalous than the cellular data (Figure 3). This result could stem from very large complexes no longer experiencing crowding effects[30] and reveals the degree of apparent anomaly resulting solely from the distribution of species in the absence of crowding effects. Alternatively, this could indicate the disintegration of complexes that coalesce *in vivo* but destabilize in the absence of molecular crowding.

4. Distribution Modeling: Decomposing Apparently Anomalous Recovery Curves into Components Exhibiting Brownian Diffusion. In any FRAP measurement, the observed signal is the sum of the signals from each species present in the sample. In a many component system, if the species have diffusion coefficients that are sufficiently different, it may be possible to distinguish distinct time scales in the recovery. More often, the observed signal takes a form that can appear as anomalous diffusion.[34,35] In our experimental systems, we observed that GFP exhibits Brownian diffusion in the interchromatin space, but Rpb3 and Rpb9 do not. There is little reason to suggest that individual proteins similar in size to GFP would exhibit true anomalous diffusion. Therefore, we investigated the possibility that each protein species is incorporated into a heterogeneous size distribution of macromolecular complexes by applying a multicomponent fit to the FRAP recovery that we term the *distribution model*.

The distribution model was implemented as[34]

$$\mathcal{F}(t) = \sum_{i=1}^{m} c_i F(D_i, t, \alpha = 1) \tag{3}$$

The recorded FRAP recovery, $\mathcal{F}(t)$, is a linear combination of Brownian diffusion basis functions, $F(D, t, \alpha = 1)$, that are given by eq 2 with $\alpha = 1$ and a range of individual diffusion coefficients. The coefficient c of each species is allowed to float and the resulting output defines a distribution of species with various diffusion coefficients (the robustness of the distribution model is detailed in Supplementary Figure 3, Supporting Information).

The distribution model was first tested by fitting the *in vivo* FRAP recovery of unconjugated GFP for an underlying distribution (Figure 5a, green). In agreement with the aforementioned fits to the anomalous diffusion model that indicated a single Brownian diffusing component, fits to the distribution model output collapsed to a Delta function, yielding a single diffusion coefficient of 27 $\mu m^2/s$ (peak 1). This is within 15% of our previously determined *in vivo* GFP diffusion coefficient.[26] Having validated the distribution model (Supplementary Figure 4, Supporting Information), we applied it to the cellular FRAP recoveries of Rpb3 and Rpb9, along with

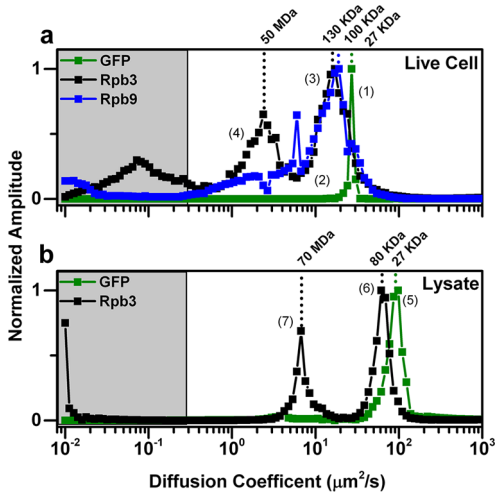

Figure 5. Brownian diffusion coefficient distributions: The distribution model (eq 4) was applied to *in vivo* (a) and (b) *in vitro* FRAP recovery curves. To implement the model, we defined 100 species with logarithmically spaced diffusion coefficients ranging from 0.20 to 1000 $\mu m^2/s$. This range of diffusion coefficients corresponds to a massive size range of species. Components with diffusion coefficients slower than 0.29 $\mu m^2/s$ are below the limit of the recovery threshold of our FRAP method. (a) The distribution of unconjugated GFP (green) collapses to a delta function with a diffusion coefficient of 27 $\mu m^2/s$. The observation of a single diffusing species demonstrates good agreement with the apparent anomalous diffusion model. The distributions for Rpb3 (black) and Rpb9 (blue) exhibit major peaks at 17 and 18 $\mu m^2/s$, respectively, corresponding to Stokes–Einstein predicted masses of 130 ± 50 and 100 ± 40 kDa, respectively. These values are in good agreement with the predicted GFP-fusion construct masses. The Rpb3 distribution is bimodal, with the slower peak indicating a diffusion coefficient of 2 $\mu m^2/s$, mapping to a mass of 50 ± 20 MDa. This peak indicates the presence of fully formed transcription factories. (b) The *in vitro* distribution for unconjugated GFP is narrow and indicates a diffusion coefficient of 92 $\mu m^2/s$, in good agreement with measurements of GFP in dilute buffer. The Rpb3 lysate distribution again reveals two well-resolved peaks, corresponding to masses of 74 ± 20 MDa and 82 ± 24 kDa, similar to the peaks in the *in vivo* measurements.

the GFP and Rpb3 lysate data. In general, the breadth of the distribution for each sample qualitatively agrees with its degree of apparent anomalous diffusion. For example, the protein exhibiting less apparent anomaly, Rpb9, exhibits a distribution of species that have Brownian diffusion coefficients in a peak from about 10 through 30 $\mu m^2/s$ (Figure 5a, red), while the Rpb3 exhibits a distribution that is even broader and more structured. However, much more information is contained in the shape of the distributions than is available from the anomaly parameter, as discussed below. Another notable observation about the distributions is that none contains diffusion components faster than unconjugated GFP.

The Stokes–Einstein equation, which predicts the diffusion coefficient of a particle undergoing Brownian diffusion, can be rearranged to estimate the relative diffusion coefficients of the proteins (assuming globular structures and the same viscosity) based on their molecular masses:

$$\frac{D_1}{D_2} = \left(\frac{M_2}{M_1}\right)^{1/3} \tag{4}$$

Here, D is the protein diffusion coefficient and M is the protein molecular mass. Using the molar mass of GFP and

dx.doi.org/10.1021/jp4082933 | J. Phys. Chem. B 2014, 118, 423–433

measured diffusion coefficient as a standard, the approximate mass corresponding to each diffusion component in the subunit distributions can be estimated using eq 4. The peak of the Rpb9 distribution (Figure 5a, peak 2) corresponds to a mass of 100 ± 40 kDa, reasonable given the 41 kDa mass of the fusion construct (we confirmed that this is independent of protein expression level, Supplementary Figure 1, Supporting Information). The width of the distribution maps to species ranging in molecular mass from 27 kDa through 10^8 kDa. While the enormous upper limit on molecular mass should be viewed with incredulity, these results indicate that species are present ranging from unconjugated GFP through aggregates of multiprotein complexes. The upper mass limit defined by the distribution is unrealistically large and likely reflects components sufficiently large to be influenced by molecular crowding that undergo true anomalous diffusion.

In contrast to Rpb9, the Rpb3 subunit exhibited a wider and more structured distribution (Figure 5a, black). Interestingly, the distribution is bimodal, with two well-resolved peaks bridged by components of lower amplitude. As expected, the fastest components are bound by an upper limit of diffusion coefficients similar to unconjugated GFP. Assuming Stokes–Einstein, the "faster" peak (Figure 5a, peak 3) corresponds to a molecular mass of 130 ± 50 kDa, in good agreement with the mass of the Rpb3-GFP fusion construct. The second, "slower" peak (Figure 5a, peak 4) corresponds to a mass of 50 ± 20 MDa. The mass of a complete transcription complex[36] consisting of RNAPII and associated transcription factors has been estimated to be ∼3 MDa; the mass of full transcription factories (aggregates of full transcription complexes and associated promoters) has been estimated up to ∼38 MDa.[1,37] Thus, the second major peak in the Rpb3 distribution is very close to the size of fully assembled gene transcription units.[1,36,37] Its presence indicates that these transcription units are present in the interchromatin space, in the absence of chromatin. We also note that the Rpb9 distribution exhibits a pronounced shoulder in the same range as the 50 MDa peak in the Rpb3 distribution.

The Rpb3 distribution also contains lower frequency components. Our FRAP method is insensitive to species slower than 0.29 $\mu m^2/s$ (explained in Supplementary Figure 2, Supporting Information). These species are likely contributions to the distribution, but the true amplitudes are uncertain. Importantly, the fit residuals are better than those produced by the anomalous diffusion model. The quality of the fits can be compared in Figures 2 and 4, where the white circles indicate the distribution model fits, in comparison to the anomalous diffusion model fits in black.

As a comparison to the *in vivo* distributions obtained for GFP and Rpb3, we applied the distribution model to the results of the lysate FRAP experiments, keeping the same number of components and the same bounds on diffusion coefficients (Figure 5b). By eliminating the stabilizing effects of macromolecular crowding, this analysis examines how the distribution of complexes is altered by a dilute environment. The distribution for the GFP lysate (Figure 5b, green) indicates a narrow range of diffusion coefficients, with the major peak indicating a diffusion coefficient of 92 $\mu m^2/s$. This is within a 10% error of the previously determined diffusion coefficient of GFP in buffer solution (84 ± 6 um^2/s),[26] confirming that the lysate provides a dilute environment that eliminates macromolecular crowding.

The results for the Rpb3 lysate (Figure 5b, black) are very similar to the distribution found *in vivo*, except shifted toward faster components due to the reduced solution viscosity. The lysate distribution indicates two major peaks, the "faster" peak at 65 $\mu m^2/s$ and the "slower" peak at 6.7 $\mu m^2/s$. These correspond to masses of 82 ± 24 kDa and 74 ± 20 MDa. Notably, the major peaks detected map to the same molecular masses as the *in vivo* fitting results, providing independent confirmation of the bimodal distribution. However, the lysate distribution differs from the *in vivo* distribution in two important respects. First, the middle range of diffusing components (intermodal) between the two peaks is absent in the lysate distribution. This change could be due to a destabilization of protein complexes that are present in the crowded nuclear environment once they are in the dilute solvent. Alternately, the preexisting equilibrium between free and complexed proteins could be shifted in favor of free species at lower protein concentrations. Regardless, the observation of species that are intermediate between complete and incomplete transcription factories has implications for the preassembly of transcription complexes. Their presence suggests that the formation of large protein assemblies proceeds through partially assembled intermediates whose formation is favored in the nuclear environment. Second, the very slow components that are technically below our FRAP resolution limit are largely absent in the lysate distribution. This supports the suspicion that those components *in vivo* represent complexes sufficiently large to experience macromolecular crowding and truly exhibit anomalous diffusion.

DISCUSSION

1. A New Perspective on in Vivo Diffusion of Macromolecule Components: Apparent Anomalous Diffusion. Our experiments with RNAPII subunits sought to directly probe the nucleoplasm, devoid of chromatin, for evidence of the holoenzyme or larger transcription complexes. We determined that RNAPII subunits exhibit complex transport dynamics even in the absence of chromatin, that can be attributed to a staggeringly large distribution of assembly states, ranging from fully assembled transcription factories to unengaged subunits. The existence of such nuclear assemblies concerns one of the current fundamental dilemmas in modern biology—determining how large DNA-binding protein complexes assemble and subsequently find their binding sites. Recent studies have supported the theory that many DNA binding complexes encounter and bind to chromatin through a stochastic diffusion-mediated process, but little evidence exists to explain what governs the assembly of these multicomponent complexes away from binding sites. Given the centrality of RNAP to transcription and possible mechanistic universality with regards to other large nuclear-localized complexes,[38] this multi-subunit complex has been the subject of great scrutiny over the past decade.

Information about the assembly and interactions of large protein complexes can be obtained by investigating transport properties of individual components, since protein mobility not in accordance with Brownian diffusion can indicate the presence of binding interactions or molecular hindrance.[27,39−41]

Given the widespread implementation of FRAP and FCS, it is interesting to note that, with very few exceptions,[33] the preponderance of eukaryotic proteins studied *in vivo* have been found to exhibit anomalous subdiffusion, while similar sized

molecules studied in aqueous or viscous solvents typically have been found to obey Brownian motion.[25,26,30,33,42−46]

We compared the transport dynamics of the RNAPII subunits Rpb3 and Rpb9 to unconjugated GFP. Suspecting that the chromatin organization of typical eukaryotic cells could pose a potential interference to diffusion mobility, we avoided confounding structures present in the nuclear environment by choosing the polytene salivary glands of *Drosophila melanogaster* larvae as our model system. The polytene cell architecture contains discrete interchromatin space devoid of genomic DNA, though it is possible that diffusing binding partners of RNAPII could be present. Our FRAP experiments performed with unconjugated GFP revealed that this inert protein is subject to Brownian diffusion. Nuclear molecular crowding was experienced as a change in viscosity resulting in a reduction of the diffusion coefficient of GFP from 84 ± 6 $\mu m^2/s$ in dilute solvent to 32 ± 6 $\mu m^2/s$ in *Drosophila* cells. In contrast to GFP, we observed apparent anomalous diffusion for both RNAPII subunits. This is very surprising as the approximately 2-fold increase in molecular mass of the fusion proteins relative to GFP would be expected to yield a very minor 1.2-fold change in diffusion coefficient based on Stokes−Einstein estimations (eq 4). This is hardly a large enough increase in size to make either subunit susceptible to extreme molecular crowding. Having eliminated all other contributions to anomalous diffusion, we have shown that molecular crowding is not a cause of anomalous diffusion for proteins in this size range. Therefore, we reason that the subunits are actually engaged in distributions of complexes displaying an extremely large range of diffusion coefficients and therefore molecular sizes. We term this phenomenon *apparent anomalous diffusion*.

Apparent anomalous diffusion was suggested in the 1990s and experimentally confirmed to affect FRAP curves by using simple two-component systems with inert solutes.[34,35,47] These previous groups demonstrated that multicomponent FRAP recovery curves of Brownian diffusing species can be represented by an anomalous fit, but this was not confirmed in a living system until now. Our experiments simultaneously probe the diffusion of assemblies with vastly different mobilities, from isolated subunits to possible aggregates of fully formed transcription units. Observed differences in the recovery dynamics of the two subunits (Figure 2) indicate that they participate in different distributions of complexes (Figure 5). This reflects differential affinities for the other RNAPII subunits and associated transcription factors, as well as suggesting that distribution width and subunit incorporation sequence are entwined.

We further explored the cellular transport behavior by performing FRAP experiments on *in vitro* lysates prepared from the GFP and Rpb3 polytene samples (Figure 4). The diluted solvent abolished macromolecular crowding and ensured that the proteins did not experience crowding effects or find binding partners. This left only a distribution of diffusing species as the remaining source of perceived anomalous diffusion.[48] The results indicate that many of the Rpb3 complexes remained intact during the lysate preparation, since it still exhibited apparent anomalous diffusion (Figure 3).

It has been reported previously that the extent of anomalous diffusion can be used as a measure for environmental heterogeneity.[25] We argue that, having shown that interchromatin space represents a homogeneous diffusive environment, the degree of anomaly can instead be a proxy for the width of the distribution in which the tagged protein participates. This makes intuitive sense—if an anomaly factor of unity represents normal diffusion and therefore a single diffusing component, any departure from unity is describing an increasingly heterogeneous mixture. We found the Rpb3 subunit was associated with the highest degree of apparent anomalous diffusion (Figure 3), indicating it participates in the widest size range of complexes (Figure 5). The Rpb9 subunit was found to exhibit less apparent anomaly (Figure 3), corresponding to a more narrow distribution (Figure 5), while GFP, which does not interact with any other species, was found to show normal diffusion.

We applied a multicomponent model to extract the underlying distributions of nuclear Rpb3 and Rpb9 to determine their participation in preassembled RNAPII complexes. The distribution model is advantageous as no *a priori* assumptions about the underlying distribution are made, thus protein complex subpopulations can be resolved. In reality, this model faces three limitations. The model assumes all component species obey Brownian diffusion—it is unable to resolve simultaneous diffusion of Brownian and anomalous species. Second, the application of the model is affected by the quality of the data. As reported by others,[34,35] the SNR of the data impacts the ability of the model to accurately resolve separate species, even in well-resolved binary systems. Our implementation is sufficient to reliably predict two components at our experimental SNR, yet the potential complexity of the protein distributions means that discerning the fine structure of subpopulations is difficult. Finally, our FRAP implementation poses a resolution limit on how slowly diffusing a species we can accurately measure.

As anticipated, the comparison of the Rpb3 and Rpb9 distributions confirms that the greater the degree of apparent anomalous diffusion (Figure 3), the wider the predicted distribution (Figure 5a). We can immediately detect that the Rpb3 subunit is involved in a wider array of complexes than Rpb9, with more of them involving very large molecular weight assemblies. The distribution modeling of the Rpb3 lysate reveals essentially the same structure, though shifted to faster diffusion components due to the reduced solvent viscosity. This provides two different experimental samples that confirm that same finding. Significantly, the more massive population is identical between both samples and corresponds to overlapping molecular mass ranges of 50 ± 20 MDa *in vivo* and 70 ± 20 MDa *in vitro*. Given the several mega-Dalton mass of a complete transcription complex[36] and the much larger mass of transcription factories,[1,37] this population represents a fully assembled transcription factory. Such complexes likely arise given the affinities between transcription complex subunits and the crowded cellular environment in which they dwell, meshing well with reports that transcription factories remain even in the absence of transcription.[49]

While the envelope shape of Rpb3 associated complexes is preserved in the lysate preparation (Figure 5), it is noteworthy that the majority of the *in vivo* distribution components lying between the major peaks are eliminated in the lysate distribution. These represent dynamic complexes that are stabilized in the crowded nuclear environment, where dissociation and rebinding is rapid due to partner proximity. In the dilute lysate solvent, once a complex of low stability dissociates, rebinding is inhibited by the low concentration of binding partner. Further, the width of both peaks is similar to the width of the GFP peak. This indicates the remaining species show less dispersion. Finally, the lysate data does not exhibit

the same structures at very slow diffusion coefficients (mapping to greater than a GDa), possibly an indication that Brownian diffusion was restored for very large complexes affected by macromolecular crowding.

2. Broad Assembly Distributions Allow for Flexibility in the Mechanism of Transcription Complex Formation. Previous work has established the dynamic turnover of RNAPI and RNAPII associated proteins during transcription. It has been shown that four subunits of RNAPI as well as several preinitiation factors all exhibit unique diffusion properties even in the vicinity of chromatin and do not diffuse as an ensemble. Further, engaged RNAPII has been found to continuously exchange with nucleoplasmic RNAPII in transcriptionally active chromatin regions.[12,13,20,50,51] These findings have led to the developing consensus that complexes assemble at a promoter site through stochastic interactions. However, the continued evidence for the formation and stability of fully assembled transcription factories even in the absence of transcription throws uncertainty on the spatiotemporal formation of such assemblies.[7,13,17,52,53] Unfortunately, previous studies could not track the dynamics of the RNAP subunits prior to recruitment or localization.

Using our method which is sensitive to the diffusion, and therefore mass of a complex, but not to the activity state, our experiments have probed the dynamics of multiple subunits within the same binding complex, enabling us to observe the degree of preassembly. This is significant as our analysis was restricted to the interchromatin space, representing a cellular location that we found to precede incorporation of all subunits into higher order assemblies but that follows subunit mRNA translation. Our work has shown that two subunits of RNAPII, including the central binding subunit Rpb3, exhibit different diffusion dynamics (Figure 2). This casts doubt on *complete* preassembly of all RNAPII substituents prior to chromatin binding.[6,7,12−17] For both subunits, we detect a subpopulation of molecular complexes approaching a limit of 100 MDa (Figure 5), which corresponds to aggregates of fully assembled transcription factories. This indicates that transcription complex subunits have high affinities that experience enhanced stability conferred by the crowded cellular environment in which they dwell.

These distributions indicate that the formation of large protein complexes is driven by stabilizing interactions even in the absence of chromatin, yet this subpopulation does not account for all of the RNAPII subunits present within the interchromatin space. This has implications for large multicomplex assembly pathways, as stochastic protein−chromatin interactions can be reframed in terms of sampling interactions between complexes in various states of completeness. Such a model is at odds with the more static, top-down view of factory formation. While our results indicate that large macromolecular complexes, such as transcription factories, are stable *in vivo*, the unanswered question is for how long they remain assembled. Most studies documenting transcription factories have relied on the appearance of punctuate structures observed in fixed cells or on the purification of stable transcription complexes *in vitro*.[4,18] Additionally, electron microscopy measurements that document the size of these complexes place an upper limit of <200 nm in diameter, still too small to accurately resolve with optical microscopy on living cells.[37] These complicating factors, combined with our findings of the stability of large protein complexes *in vitro*, make it difficult to determine the longevity of these species. Further, while our study was able to characterize diffusive behavior in discrete nuclear regions, we are not yet able to discern the potential activity of large transcription complexes. Thus, a portion of the detected population may contain complete transcription complexes that have been aborted and are unable to initiate transcription.

As investigations into the dynamics of polymerase components and associated transcription factors reveal a conserved intrinsic turnover and universally accepted inefficiency of transcription initiation, the previously posited model of stochastic gene expression has gained traction.[7,52] Mounting evidence indicates that RNAPII is not always recruited as a holoenzyme, though our findings indicate that full transcription factories do form prior to RNAPII recruitment.[52] Despite evidence for factory mechanisms, RNAPII is currently seen as assembling at a promoter through a multistep process marked by efficient chromatin capture rates of up to 50%[13] but highly inefficient transcription initiation (<1%),[14] leading to an overall transient promoter interaction prior to elongation (which is unlikely if full transcription factories migrated the entire nucleus).

We believe our findings of RNAPII subunits existing in complex distributions lend validity to both models. Our essential finding is that transcription subunits form large, stable, and mobile complexes, indicating the true assembly behavior lies midway on a spectrum of preassembly. We measured diffusion coefficients for transcription factories in line with those determined for other proteins involved in nuclear macromolecular assemblies.[50] This suggests that large complexes are mobile (but slow) and can diffuse to binding sites, in contrast to static factory models in which chromatin must migrate to stationary factories. This integrates well with current observations but helps to redefine the nature of assembly. Our results provide experimental evidence to considerations proffered by Phair and Misteli that protein complexes can form stochastically, distal to their site of action, enabling rapid recruitment and dynamic responses to changes in binding partner availability.[7,50−52] However, the large population of individual subunits and partially formed complexes also allows for *de novo* assembly at gene loci.

As opposed to a hit-and-run model of polymerase factors encountering a chromatin binding site, our findings show that transcription complexes assemble to varying levels of completion in the interchromatin space removed from and prior to encountering chromatin. These partially formed assemblies, through diffusion, experience stochastic encounters with potential binding sites, with the duration of the encounter depending on the completeness of the polymerase assembly. It is then possible that more complete RNAPII complexes, having a greater compliment of binding partners, form more stable chromatin interactions than less well developed subassemblies. As our distribution modeling shows, the majority of the subunits exist as incomplete assemblies; therefore, the majority of chromatin interactions are likely aborted, leading to the inefficiency of transcription initiation. Our observation of a bias toward larger complexes exhibited by the more massive RNAPII Rpb3 (Figure 5) subunit may reveal a measure of stepwise assembly. In this scenario, the larger subunits complex first, leading to stable chromatin-binding assemblies, forming nucleation sites for smaller subunit assemblies. Such a model ensures maximum flexibility in gene expression for different chromatin regions. The two assembly regimes we observe mean that fully formed transcription complexes, in the presence of open chromatin regions, are likely to remain stably assembled

and engage in high throughput transcription. These large structures experience slow diffusion and would remain relatively stationary, in alignment with transcription factory theory. Conversely, the smaller subassembled modules, which account for a large fraction of the assembly states, are capable of rapid diffusion and permit protein recruitment to congested chromatin regions that experience lower basal transcription levels. The partial preassembly of the transcription complex enhances the efficiency of full complex assembly and is complimented by greater nuclear mobility than near-immobile transcription factories. Thus, through a partially modular assembly mechanism, the cell is endowed with a flexible response to changing transcription demands.

Additionally, while not the focus of this work, we have previously observed true anomalous diffusion due to confinement in the vicinity of the chromatin lattice even for small proteins.[26] Coupled with the findings of other researchers concerning the role of molecular crowding in gene expression,[54−56] it stands to reason that large, partially assembled complexes, once in the vicinity of a promoter, sample increasingly frequent binding events due to molecular confinement and reduced mobility.

CONCLUSION

By applying FRAP in the polytene salivary glands of *Drosophila melanogaster* as a model system, we show for the first time that RNAPII exists in a large distribution of partially assembled complexes in the interchromatin space, including fully assembled transcription factories. Having determined that the Rpb3 and Rpb9 subunits exhibit different diffusion properties, we confirm that RNAPII is a dynamic complex, though we detect a population of complete preassembled transcription factories prior to chromatin binding. Using GFP as an inert internal control protein, we have shown *in vivo* that the subunit distributions display apparent anomalous diffusion. This arises from the simultaneous interrogation of multiple diffusing species using an ensemble measurement method. When considered individually, these complexes move primarily by Brownian diffusion throughout the crowded interchromatin space, experiencing a reduction in mobility due to the high viscosity but not experiencing molecular confinement. We confirmed the existence of these subunit assembly distributions through the use of cell lysates, in which apparent anomalous diffusion persisted in the absence of macromolecular crowding. The discovery of these partially assembled RNAPII complexes helps integrate current contradictory observations regarding the mode of transcription complex assembly. Our findings are consistent with the simultaneous action of a top-down and bottom-up assembly. While the exact nature of the species that initiate transcription cannot yet be determined, for the first time, our data shows evidence for a distribution of preassembled complexes. Finally, the distribution of assembly states suggests that a partially modular mechanism of macromolecular assembly enables a flexible response to gene transcription.

MATERIALS AND METHODS

All chemicals are Fisher brand unless noted.

1. Fly Strains. *Drosophila* lines that express Rpb3-GFP, Rpb9-GFP, or H2B-mRFP using the GAL4/UAS system have been described previously.[28,53] Fly lines containing transgenes for unconjugated GFP and Gal4-C147 were obtained from the Bloomington Drosophila Stock Center (lines #5430 and #6979, respectively). All GFP samples are enhanced green fluorescent protein. To simultaneously express H2B-mRFP with GFP or GFP fusions for dual color imaging, the homozygous line Gal4-C140; H2B-mRFP was first generated and then crossed to the appropriate GFP fusion transgenic line. Flies were raised using a standard cornmeal medium at room temperature; larvae were collected after 8−9 days. To prepare samples for imaging, wandering third-instar larvae were dissected in Grace's Insect Medium and intact salivary glands were used for imaging polytene cells. All imaging experiments were completed within 1 h of dissection to maintain cell viability.

2. Salivary Gland Extract Preparation. To prepare polytene cellular extract samples of GFP and EGFP-Rpb3, 80 larvae were dissected and the glands placed on ice cold Tris buffer (50 mM, pH 7.4). The glands were mini-centrifuged for 60 s, the supernatant removed, and the glands resuspended in ice cold lysis buffer (50 μL), followed by vortexing for 45 s and sonication for 30 min to rupture the glands. The lysis buffer consisted of Tris−HCl (50 mM, pH 7.4), NaCl (150 mM), NP-40 detergent (0.5% w/v), Pefabloc SC (1 mM in Tris buffer), leupeptin (2 μg/mL, in methanol), and pepstatin (2 μg/mL, in methanol). After sonication in ice cold lysis buffer, the sample was mini-centrifuged for 4 min. The supernatant was used immediately for FRAP experiments.

3. Two-Photon Microscopy Configuration and FRAP Procedures. Imaging and FRAP were done as described in our previous paper.[26] In brief, polytene cells were imaged with a 1.2NA/60× Olympus objective using a home-built laser scanning two-photon microscope. GFP and RFP were excited at 950 nm by a Chameleon Ultra II Ti:sapphire pulsed laser with a 140 fs pulse duration; the fluorophore emissions separated with a 570 short pass dichroic mirror. The GFP emission was collected with a 510/30 bandpass filter, while RFP emission was collected with a 630/100 dichroic mirror. Quantitative bleaching studies were performed with a point-bleaching method (ptFRAP) developed previously in our laboratory, featuring an online image thresholding and data acquisition procedure followed by offline image analysis and data modeling. For all conditions studied, between 20 and 40 cells were analyzed; the number of data points collected and averaged are indicated in Figures 2 and 4. Data collection consists of two phases—recording bleach and control data points. Bleach points are established by photobleaching a diffraction limited volume (spot size of 300 nm diameter and 1 μm axial length) at a high laser power (bleach power) followed by recording the intensity of the spot during the diffusive recovery at a lower laser power (read power). Control points are established in the same manner but with the read power used in place of the bleaching power. A bleach depth of between 40 and 60% of the initial fluorescent intensity was achieved using a bleach power of 71.5 mW, while control measurements were taken at a read power of 11.5 mW (both values measured at the microscope objective using a calibrated power meter). For all proteins studied, FRAP recovery data was collected for 50 ms and data fitting was applied to data points collected starting at 80 μs postbleach. The data was fit with a model for anomalous subdiffusion,[26] which indicates the degree of anomaly and the diffusion coefficient (for normally diffusing species) or the transport coefficient of the diffusing species. The anomaly factor ranges between 1 and 0, with unity indicating Brownian diffusion. For detailed information on the microscope configuration, FRAP timing sequence, and fitting

dx.doi.org/10.1021/jp4082933 | J. Phys. Chem. B 2014, 118, 423−433

recovery data to an anomalous subdiffusion model with a photophysics correction for observational photobleaching, see Daddysman and Fecko.[26]

■ ASSOCIATED CONTENT

Supporting Information

Four figures detailing specifics concerning the FRAP analysis and modeling and a table detailing the fitting results for individual data sets prior to ensemble treatment. This material is available free of charge via the Internet at http://pubs.acs.org.

■ AUTHOR INFORMATION

Corresponding Author

*E-mail: cfecko@unc.edu. Fax: 919-962-2388. Phone: 919-962-052.

Author Contributions

C.J.F., M.K.D., and M.A.T. conceived the study and designed experiments. M.A.T. designed the automated FRAP collection programs. M.A.T. collected the data for the Rpb3 and Rpb9 FRAP curves. M.K.D. collected the data for GFP FRAP curves. C.J.F. and M.K.D. were the primary architects of the distribution modeling implement. M.A.T. wrote the manuscript with support from C.J.F. and M.K.D.

Notes

The authors declare no competing financial interest.

■ ACKNOWLEDGMENTS

Funding for this work was provided by the National Science Foundation under Grant No. PHY-1150017.

■ REFERENCES

(1) Melnik, S.; Deng, B.; Papantonis, A.; Baboo, S.; Carr, I. M.; Cook, P. The proteomes of transcription factories containing RNA polymerases I,II, or III. *Nat. Methods* **2012**, *8*, 963.

(2) Kruhlak, M. J.; Lever, M. A.; Fischle, W.; Verdin, E.; Bazett-Jones, D. P.; Hendzel, M. J. Reduced Mobility of the Alternate Splicing Factor (Asf) through the Nucleoplasm and Steady State Speckle Compartments. *J. Cell Biol.* **2000**, *150*, 41−52.

(3) Meister, P.; Poldevin, M.; Francesconi, S.; Tratner, I.; Zarzov, P.; Baldacci, G. Nuclear factories for signally and repairing DNA double strand breaks in living fission yeast. *Nucleic Acids Res.* **2003**, *31*, 5064.

(4) Hemmerich, P. Assessing protein dynamics in the cell nucleus. *Zellbiologie* **2005**, *31*, 18.

(5) Houtsmuller, A. B.; Vermeulen, W. Macromolecular dyanmics in living cell nuclei reveals by fluorescence redistribution after photobleaching. *Histochem. Cell Biol.* **2001**, *115*, 13.

(6) Cook, P. R. A Model for all Genomes: The Role of Transcription Factories. *J. Mol. Biol.* **2010**, *395*, 1−10.

(7) Misteli, T. Protein dynamics: Implications for nuclear architecture and gene expression. *Science* **2001**, *291*, 843−847.

(8) Hahn, S. Structure and mechanism of the RNA polymerase II transcription machinery. *Nat. Struct. Mol. Biol.* **2004**, *11*, 394−403.

(9) Davis, J. A.; Takagi, Y.; Kornberg, R. D.; Asturias, F. J. Structure of the Yeast RNA Polymerase II Holoenzyme: Mediator Conformation and Polymerase Interaction. *Mol. Cell* **2002**, *10*, 409−415.

(10) Woychik, N. A.; Hampsey, M. The RNA Polymerase II Machinery: Structure Illuminates Function. *Cell* **2002**, *108*, 453−463.

(11) Cramer, P.; Bushnell, D. A.; Kornberg, R. D. Structural Basis of Transcription: RNA Polymerase II at 2.8 Ångstrom Resolution. *Science* **2001**, *292*, 1863−1876.

(12) Gorski, S. A.; Snyder, S. K.; John, S.; Grummt, I.; Misteli, T. Modulation of RNA Polymerase Assembly Dynamics in Transcriptional Regulation. *Mol. Cell* **2008**, *30*, 486−497.

(13) Dundr, M.; Hoffmann-Rohrer, U.; Hu, Q.; Grummt, I.; Rothblum, L. I.; Phair, R. D.; Misteli, T. A Kinetic Framework for a Mammalian RNA Polymerase in Vivo. *Science* **2002**, *298*, 1623−1626.

(14) Darzacq, X.; Shav-Tal, Y.; de Turris, V.; Brody, Y.; Shenoy, S. M.; Phair, R. D.; Singer, R. H. In vivo dynamics of RNA polymerase II transcription. *Nat. Struct. Mol. Biol.* **2007**, *14*, 796−806.

(15) Yao, J.; Ardehali, M. B.; Fecko, C. J.; Webb, W. W.; Lis, J. T. Intranuclear distribution and local dynamics of RNA polymerase II during transcription activation. *Mol. Cell* **2007**, *28*, 978−990.

(16) Chen, D.; Dundr, M.; Wang, C.; Leung, A.; Lamond, A.; Misteli, T.; Huang, S. Condensed mitotic chromatin is accessible to transcription factors and chromatin structural proteins. *J. Cell Biol.* **2005**, *168*, 41−54.

(17) Schneider, D. A.; Nomura, M. RNA polymerase I remains intact without subunit exchange through multiple rounds of transcription in Saccharomyces cerevisiae. *Proc. Natl. Acad. Sci. U.S.A.* **2004**, *101*, 15112−15117.

(18) Hannan, R. D.; Cavanaugh, A.; Hempel, W. M.; Moss, T.; Rothblum, L. Identification of a mammalian RNA Polymerase I holenezyme containing components of the DNA repair/replication system. *Nucleic Acids Res.* **1999**, *27*, 3720.

(19) Grummt, I. Life on a planet of its own: regulation of RNA Polymerase I transcription in the nucleolus. *Genes Dev.* **2003**, *17*, 1691.

(20) Kimura, H.; Sugaya, K.; Cook, P. R. The transcription cycle of RNA polymerase II in living cells. *J. Cell Biol.* **2002**, *159*, 777−782.

(21) Politi, A.; Moné, M. J.; Houtsmuller, A. B.; Hoogstraten, D.; Vermeulen, W.; Heinrich, R.; van Driel, R. Mathematical Modeling of Nucleotide Excision Repair Reveals Efficiency of Sequential Assembly Strategies. *Mol. Cell* **2005**, *19*, 679−690.

(22) Ishikawa-Ankerhold, H. C.; Ankerhold, R.; Drummen, G. P. C. Advanced Fluorescence Microscopy Techniques—FRAP, FLIP, FLAP, FRET and FLIM. *Molecules* **2012**, *17*, 4047−4132.

(23) Yao, J.; Zobeck, K. L.; Lis, J. T.; Webb, W. W. Imaging transcription dynamics at endogenous genes in living Drosophila tissues. *Methods* **2008**, *45*, 233−241.

(24) Lis, J. T. Imaging Drosophila gene activation and polymerase pausing in vivo. *Nature* **2007**, *450*, 198−202.

(25) Weiss, M.; Elsner, M.; Kartberg, F.; Nilsson, T. Anomalous Subdiffusion Is a Measure for Cytoplasmic Crowding in Living Cells. *Biophys. J.* **2004**, *87*, 3518−3524.

(26) Daddysman, M. K.; Fecko, C. J. Revisiting Point FRAP to Quantitatively Characterize Anomalous Diffusion in Live Cells. *J. Phys. Chem. B* **2013**, *117*, 1241−1251.

(27) Sprague, B. L.; McNally, J. G. FRAP analysis of binding: proper and fitting. *Trends Cell Biol.* **2005**, *15*.

(28) Zobeck, K. L.; Buckley, M. S.; Zipfel, W. R.; Lis, J. T. Recruitment Timing and Dynamics of Transcription Factors at the Hsp70 Loci in Living Cells. *Mol. Cell* **2010**, *40*, 965−975.

(29) Acker, J.; de Graaff, M.; Cheynel, I.; Khazak, V.; Kedinger, C.; Vigneron, M. Interactions between the Human RNA Polymerase II Subunits. *J. Biol. Chem.* **1997**, *272*, 16815−16821.

(30) Seksek, O.; Biwersi, J.; Verkman, A. S. Translational diffusion of macromolecule-sized solutes in cytoplasm and nucleus. *J. Cell Biol.* **1997**, *138*, 131−142.

(31) Sokolov, I. M. Models of anomalous diffusion in crowded environments. *Soft Matter* **2012**, *8*, 9043−9052.

(32) Brown, E. B.; Wu, E. S.; Zipfel, W. R.; Webb, W. W. Measurement of Molecular Diffusion in Solution by Multiphoton Fluorescence Photobleaching Recovery. *Biophys. J.* **1999**, *77*, 2837−2849.

(33) Dix, J. A.; Verkman, A. S. Crowding Effects on Diffusion in Solutions and Cells. *Annu. Rev. Biophys. Biomol. Struct.* **2008**, *37*, 247.

(34) Periasamy, N.; Verkman, A. S. Analysis of Fluorphore Diffusion by Continuous Distributions of Diffusion Coefficients: Application to Photobleaching Measurements of Multicomponent and Anomalous Diffusion. *Biophys. J.* **1998**, *75*, 557.

(35) Gordon, G. W.; Chazotte, B.; Wang, X. F.; Herman, B. Analysis of Simulated and Experimental Fluorescence Recovery After Photo-

bleaching. Data for Two Diffusing Components. *Biophys. J.* **1995**, *68*, 766.
(36) Wilson, C. J.; Chao, D. M.; Imbalzano, A. N.; Schnitzler, G. R.; Kingston, R. E.; Young, R. A. RNA Polymerase II Holoenzyme Contains SWI/SNF Regulators Involved in Chromatin Remodeling. *Cell* **1996**, *84*, 235−244.
(37) Eskiw, C.; Fraser, P. Ultrastructural study of transcription factories in mouse erythroblasts. *J. Cell Sci.* **2011**, *124*, 3676.
(38) Hager, G.; Elbi, C.; Becker, M. Protein dynamics in the nuclear compartment. *Curr. Opin. Genet. Dev.* **2002**, *12*, 137.
(39) Mueller, F.; Wach, P.; McNally, J. G. Evidence for a Common Mode of Transcription Factor Interaction with Chromatin as Revealed by Improved Quantitative Fluorescence Recovery after Photobleaching. *Biophys. J.* **2008**, *94*, 3323−3339.
(40) Feder, T. J.; Burst-Mascher, I.; Slattery, J. P.; Baird, B.; Webb, W. W. Constrained diffusion or immobile fraction on cell surfaces: A new interpretation. *Biophys. J.* **1996**, *70*, 2767−2773.
(41) Malchus, N.; Weiss, M. Elucidating Anomalous Protein Diffusion in Living Cells with Fluorescence Correlation Spectroscopy-Fatcs and Pitfalls. *J. Fluoresc.* **2010**, *20*, 19.
(42) Fushimi, K.; Verkman, A. S. Low viscosity in the aqueous domain of cell cytoplasm measured by picosecond polarization microfluorimetry. *J. Cell Biol.* **1991**, *112*, 719−725.
(43) Mika, J. T.; Poolman, B. Macromolecule diffusion and confinement in prokaryotic cells. *Curr. Opin. Biotechnol.* **2011**, *22*, 117−126.
(44) Bancaud, A.; Huet, S.; Daigle, N.; Mozziconacci, J.; Beaudouin, J.; Ellenberg, J. Molecular crowding affects diffusion and binding of nuclear proteins in heterochromatin and reveals the fractal organization of chromatin. *EMBO J.* **2009**, *28*, 3785−3798.
(45) Wu, J.; Corbett, A. H.; Berland, K. M. The Intracellular Mobility of Nuclear Import Receptors and NLS Cargoes. *Biophys. J.* **2009**, *96*, 3840−3849.
(46) Guigas, G.; Kalla, C.; Weiss, M. The degree of macromolecular crowding in the cytoplasm and nucleoplasm of mammalian cells is conserved. *FEBS Lett.* **2007**, *581*, 5094−5098.
(47) Hauser, G. I.; Seiffert, S.; Oppermann, W. Systematic evaluation of FRAP experiments performed in a confocal laser scanning microscope? Part II: Multiple diffusion processes. *J. Microsc.* **2008**, *230*, 353−362.
(48) Stasevich, T. J.; Mueller, F.; Michelman-Ribeiro, A.; Rosales, T.; Knutson, J. R.; McNally, J. G. Cross-Validating FRAP and FCS to Quantify the Impact of Photobleaching on In Vivo Binding Estimates. *Biophys. J.* **2010**, *99*, 3093−3101.
(49) Mitchell, J. A.; Fraser, P. Transcription factories are nuclear subcompartments that remain in the absence of transcription. *Genes Dev.* **2008**, *22*, 20.
(50) Phair, R. D.; Misteli, T. High mobility of proteins in the mammalian cell nucleus. *Nature* **2000**, *404*, 604.
(51) Hager, G.; McNally, J. G.; Misteli, T. Transcription Dynamics. *Mol. Cell* **2009**, *35*, 741.
(52) Misteli, T. Beyond the Sequence: Cellular Organization of Genome Function. *Cell* **2007**, *128*, 787.
(53) Yao, J.; Munson, K. M.; Webb, W. W.; Lis, J. T. Dynamics of heat shock factor association with native gene loci in living cells. *Nature* **2006**, *442*, 1050−1053.
(54) Guigas, G.; Weiss, M. Sampling the Cell with Anomalous Diffusion—The Discovery of Slowness. *Biophys. J.* **2008**, *94*, 90−94.
(55) Hancock, R. A role for macromolecular crowding effects in the assembly and function of compartments in the nucleus. *J. Struct. Biol.* **2004**, *146*, 281−290.
(56) Minton, A. P. Implications of macromolecular crowding for protein assembly. *Curr. Opin. Struct. Biol.* **2000**, *10*, 34−39.